[Frontiers In Bioscience, Elite, 9, 192-203, March 1, 2017]

Biphasic organo-bioceramic fibrous composite as a biomimetic extracellular matrix for bone tissue regeneration

Sanjay Kumar[1], James A. Stokes III[1], Derrick Dean[2], Christian Rogers[3], Elijah Nyairo[3], Vinoy Thomas[4], Manoj K. Mishra[1]

[1]Cancer Biology Research and Training Program, Department of Biological Sciences, [2]Biomedical Engineering, Alabama State University, Montgomery, AL 36104, USA, [3]Physical Sciences, Alabama State University, Montgomery, AL 36104, USA, [4]Department of Material Science and Engineering, University of Alabama, Birmingham, AL USA

TABLE OF CONTENTS

1. ABSTRACT

In bone tissue engineering, the organo-ceramic composite, electrospun polycaprolactone/hydroxyapatite (PCL/HA) scaffold has the potential to support cell proliferation, migration, differentiation, and homeostasis. Here, we report the effect of PCL/HA scaffold in tissue regeneration using human mesenchymal stem cells (hMSCs). We characterized the scaffold by fourier transform infrared spectroscopy (FTIR), differential scanning calorimetry (DSC), scanning electron microscope (SEM) and assessed its biocompatibility. PCL/HA composite is superior as a scaffold compared to PCL alone. Furthermore, increasing HA content (5-10%) was more efficacious in supporting cell-scaffold attachment, expression of ECM molecules and proliferation. These results suggest that PCL/HA is useful as a scaffold for tissue regeneration.

2. INTRODUCTION

Recent advances in bone tissue engineering provide a new dimension and promising approach to treat harmful conditions associated with bones (1). Bone is a natural composition of organic (approximately 90%) fibrils of collagens (Type I, II, III, and IV), fibronectin, laminin, tenascin, and vitronectin and inorganic molecules (such as hyaluronic acid or HA [Ca_{10} $(OH)_2$ $(PO_4)_6$] that serve as the bone matrix. All of which are embedded in a well-organized, well-arrayed nanocrystalline and rod-like inorganic material with a length of 25-50 nm (2, 3). Bone is the second most transplantable tissue in the body, which is extensively used in orthopedic applications (4). Due to its high bioactivity, biocompatibility, and bio-integration, HA, has traditionally been used as a bio-ceramic filler in polymer-based bone substitutions (5, 6). Moreover, HA shows close affinity to many adhesive proteins and contributes directly to osteoclast defense

and mineralization (7, 8). Synthetic hydroxyapatite (HA) exhibits similar chemical composition to the inorganic minerals of natural bone, and thus may be ideal as a bone substitute in biomedical applications (9, 10). However, studies have demonstrated that HA exhibits poor mechanical properties, including high brittleness and low elasticity thus limiting its application directly as a bone substitute in the bone tissue engineering (9, 10). In view of this, synthesis and characterization of nano sized HA have received intensive interest in nanoscience and nanotechnology (11, 12). However, it needs a supportive biodegradable skeleton such as polycaprolactone (PCL) fibers. Thus PCL/HA composite nanofibers are attractive for tissue scaffold applications.

Polycaprolactone (PCL) is a biodegradable, recyclable, polyester with remarkable toughness and biocompatibility (13). Furthermore, it is a highly flexible semi-crystalline aliphatic polymer with hydrophobicity and potent mechanical strength, and has a slower degradation rate with high fracture energy as compared to biopolymers such as starch, cellulose, and chitin (13).

An ideal porous scaffold for bone tissue engineering should be biocompatible, biodegradable, flexible, and absorbable. In addition, best-suited scaffold(s) should have good porosity, pore size, and interconnections between pores. Furthermore, a scaffold should have sufficient mechanical strength and facilitate good cell-scaffold interactions (14, 15). The combination of bioactive ceramics and biodegradable polyester to produce three-dimensional scaffolds with high porosity is an emerging idea for designing and developing novel composite systems for bone tissue regeneration (14, 15). Bone tissue engineering scaffolds were previously synthesized as composites, by the introduction of HA nanoparticles within polymeric matrices or by the mineralization of HA-nanoparticles on the surface of polymeric substances (11). However, researchers found that PCL alone showed high hydrophobicity, poor surface wetting and interactions with biological fluids, and displayed an aversion to cell adhesion and proliferation (2, 3). PCL is often used as a polymer matrix in nanocomposites such as osteogenic and osteoinductive inorganic phages, such as HA to confer its high bioactivity to the polymer based composite stimulating bone regeneration. Thus, electrospun scaffold(s) shows greater efficiency as compared to pure HA (6). In addition, scaffolds after HA applications were able to maintain their mechanical properties for an appropriate duration (16, 17). This suggests that PCL/HA application may preserve scaffold structural stability and enhance its efficiency. Moreover, HA particles demonstrated poor interfacial adhesion when dispersed in polymer matrix due to a different chemical nature and surface energy, and results in degradation of the mechanical properties to the composite.

The goal of this investigation was to prepare and characterize a polymer-ceramic composite by introducing different concentrations of HA with *in vitro* biocompatibility of the characterized organo-ceramic composite. To achieve this goal, Neat-PCL, PCL/HA (1%, 5%, and 10%) scaffolds were synthesized using electrospinning methods. Organo-ceramic composites were characterized using FTIR, DSC, and SEM. In addition, the biocompatibility of the composite was evaluated on hMSCs by performing following assays: cellular proliferation, colorimetric (ECM cell the adhesion molecules) and cell spreading. Morphological studies were also performed. A clear-cut difference in heat flow scans and absorbances were observed between Neat-PCL and PCL/HA (1%, 5%, and 10%) using DSC and FTIR respectively. Furthermore, cell proliferation/differentiation, cell spreading, cell morphology, and the expression of ECM cell adhesion molecules were higher as compared with the control.

3. MATERIALS AND METHODS

3.1. Reagents

The bone-marrow derived human mesenchymal stem cells (hMSCs), its culture media, fetal bovine serum (FBS), L-Alanyl-L-Glutamine, Insulin-like Growth Factor-1, basic Fibroblast Growth Factor, and 3-(4,5-dimethylthiazol-2-yl)-2,5-diphenyltetrazolium bromide were obtained from American Type Culture Collection (ATCC, VA, USA). Acridine orange and propidium iodide working solution, ECM cell adhesion array kit (colorimetric; ECM540) for collagen-I, II, and IV, fibronectin, laminin, tenascin, and vitronectin were obtained from ThermoFisher Scientific (MA, USA). All other chemicals stated were either purchase from Sigma (MO, USA) or Thermo Fisher Scientific (MA, USA).

3.2. Electrospinning of scaffolds

Solutions of PCL were prepared by dissolving PCL pellets (Lactel Polymers, Hoover, AL) in a solvent (chloroform: methanol = 3:1 v/v) to achieve a 15-wt.% solution and electrospun at a high voltage of 15 kV (M826, Gamma High-Voltage Research, Ormond Beach, FL) to create Neat-PCL. A feeding rate of PCL solution 2 mL/h was set in a syringe pump (KD Scientific, Holliston, MA) and a grounded aluminum collector plate was placed approximately 12 cm from the tip of the needle. To make composite fibers of PCL with HA, HA nanoparticle powder (~100 nm particle size and 15 m^2/g surface area, Nanocerox Inc., Ann Arbor, MI, USA) of desired amount (wt.%) was dispersed in the solvent system using a magnetic stirrer for 30 min. The PCL was then dissolved, and the solution was electrospun. The spinning parameters such as the electric field, feed rate and distance between the needle and the collector were also kept the same for

the electrospinning of Neat-PCL. The mesh removed from aluminum was dried at room temperature and kept for 1 week in a desiccator to evaporate from any residual solvent. Samples were denoted as Neat-PCL and PCL/HA (at 1%, 5%, and 10% concentrations).

3.3. Characterization of scaffolds

3.3.1. Morphology and pore dimensions

For morphological studies, organo-ceramic composite fibers, Neat-PCL and PCL/HA (1%, 5%, and 10%) were cut with a razor blade accordingly and processed for SEM analysis. The organo-ceramic composites were sputter coated with gold and morphology was observed under SEM (Philips SEM 510) at an accelerating voltage of 10 kV.

The apparent density and porosity of the scaffolds were determined as per our previous publications (18), using the equations below:

$$\text{Apparent Density of the Scaffold (g/cm3)} = \frac{\text{Mass of the Scaffold (mg)}}{\text{Thickness (µm)} \times \text{Area (cm2)}}$$

$$\text{Porosity of the Scaffold (\%)} = \left(1 - \frac{\text{Apparent density}}{\text{Bulk density}}\right) \times 100$$

3.3.2. Fourier Transform Infrared Spectroscopy (FTIR) analysis

FTIR measurements of Neat-PCL and composite fibers (1%, 5%, and 10%) of PCL/HA were obtained using a Nicolet IS 50 Infrared Spectrometer in ATR mode, operating at a range from 4000 cm^{-1} to 400 cm^{-1}. To obtain a good signal/noise ratio, 512 scan per sample were recorded. Percent absorption values were plotted on the y-axis and values of wavelength (cm^{-1}) on the x-axis.

3.3.3. Differential Scanning Calorimetric (DSC) analysis

Differential scanning calorimetric (DSC) measurements of composite fibers were obtained in N_2 atmosphere at a ramp rate of 10 ^{0}C/min to 100 ^{0}C using DSC instrument (DSC Q 2000, TA Instruments, Inc., DE). Neat-PCL and composites (1%, 5%, and 10%) of PCL/HA were weighed (15 mg) in aluminum pans, scanned under the aforementioned parameter in a Q2000 DSC (TA instruments).

3.4. Determination of *in vitro* biocompatibility

3.4.1. Cell culture

Human mesenchymal stem cells (hMSCs) were obtained from American Tissue Culture Collection (ATCC; VA, USA), and were maintained in ATCC formulated culture medium supplemented with 7% fetal bovine serum (FBS), 2.4 mM of L-Alanyl-L-Glutamine, 15 ng/mL of Insulin-like Growth Factor-1, basic Fibroblast Growth Factor 125 pg/mL in 5% CO2 at 37 ^{0}C. Cells were grown up to 80-90% confluency after 2-3 passes, and thereafter cells were harvested by trypsinization, counted, and subjected to experimentation. The hMSCs were also cryopreserved for future references.

3.4.2. Cell proliferation

To assess the effect of different concentration of the organo-ceramic composite PCL/HA on cellular proliferation, the hMSCs (10^4 cells/well) were seeded into each well of a 96-well plate with Neat-PCL, PCL/HA-1%, PCL/HA-5%, and PCL/HA-10% for 48 h in 5% CO_2 at 37 ^{0}C. After 48 h of incubation, 10 µL of (5mg/ml) MTT (3-(4, 5-dimethylthiazol-2-yl)-2,5diphenyltetrazolium bromide) was added to each well of the 96-well plate and incubated for 4-5 h in 5% CO_2 at 37 ^{0}C. Before reading absorbance, 100 µL of DMSO (99.99%) was added to each well to stop the reaction. Absorbance was read at 570 nm using a microplate reader (Chromate, FL, USA).

3.4.3. Cell morphology and apoptosis

The hMSCs were harvested after trypsinization, counted, and incubated with organo-ceramic composite, Neat-PCL, PCL/HA-1%, PCL/HA-5%, and PCL/HA-10% for 48 h in 5% CO_2 at 37 ^{0}C. Cells were fixed and permeabilized with 4% formaldehyde solution for 15 min at 4 ^{0}C. Cells were then stained with acridine orange and counterstained with propidium iodide for 15 min at room temperature. Thereafter, cells were washed gently with DPBS, mounted with glycerol, and observed under a fluorescent microscope (Nikon Eclipse TE2000, NY, USA). The percentage of apoptotic cells can be determined as follows:

$$\text{Apoptotic cells(\%)} = \frac{\text{Live cells+Dead cells with apoptotic nuclei}}{\text{Dead cells with normal nuclei+Live cells+Dead cells with apoptotic nuclei}} \times 100$$

3.4.4. ECM Cell adhesion assay

To test the expression of ECM cell adhesion molecules, hMSCs were incubated at different concentrations (cited previously) of the organo-ceramic composite fibers for 48 h in 5% CO_2 at 37 ^{0}C. Cells in the presence of Neat-PCL served as the control. Cells were then harvested, counted, and 100 µl of 1×10^6 cells/mL (single cell suspension) was seeded to each well of the pre-hydrated 96-well plate (provided with ECM cell adhesion array kit) and incubated for 1-2 h at 37 ^{0}C in 5% CO_2. After incubation, media was gently aspirated from each well and washed 2-3 times with 200 µL per well of assay buffer. During aspiration 25-50 µL of wash solution was left in each well so that the cells remained hydrated at all times. After washing,

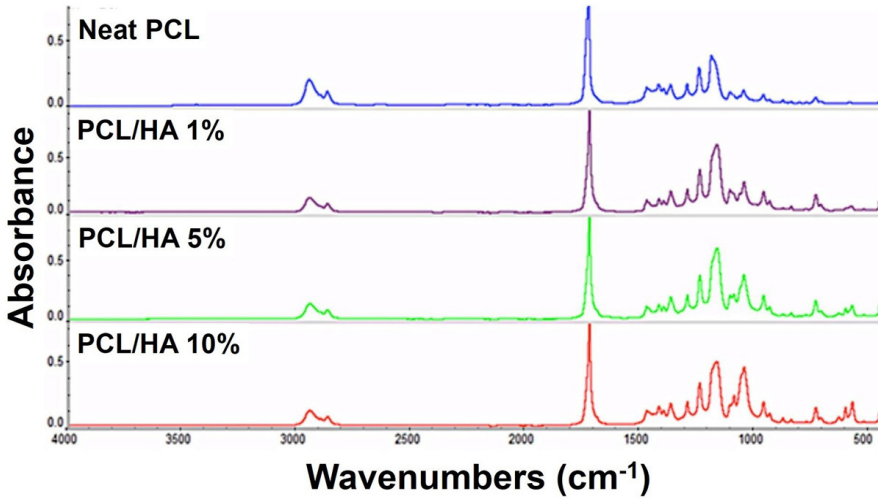

Figure 1. FT-IR scans of Neat-PCL and samples containing 1%, 5%, and 10% wt.% of HA respectively. The spectra were recorded in ATR mode from 4000 cm-1 to 400 cm-1 range at the resolution of 512 scans per sample. FTIR data clearly indicate an increase in the peak-intensity of phosphate groups at 1050 cm-1 and at 561 cm-1 with respect to an increase in HA weight % in scaffolds.

100 µL of cell stain solution was added to each well and incubated for 5 min at room temperature. After stain solution was removed, cells were then washed gently 3-5 times with MQ-water and each well was air dried for a few seconds. Thereafter, 100 µL of extraction buffer was added to each well, and incubated for 10 min on a rotating shaker at room temperature. Absorbance was read at 540 nm in reference to the 570 nm using a microplate reader (Chromate, FL, USA).

3.4.5. Cell spreading assay

Fluorescent microscopy was used to study the spreading behavior of hMSCs on the composite fibers. The hMSCs were cultured with the composite fibers. After incubation, cells were washed with DPBS in the culture plate without further trypsinization and stained with acridine orange for 15 min at room temperature. Next, staining solution was gently aspirated, cells were washed twice with DPBS and 50 µL of DPBS was added to each well in order to keep cells hydrated. Cells were observed under a fluorescent microscope (Nikon Eclipse TE2000, NY, USA).

3.5. Statistical analysis

Statistical analysis of three independent experiments in triplicates was carried out using One-way analysis of variance (ANOVA). Data was considered significant at $p<0.05$ as applicable. All statistical analysis was performed using Sigma plot version 12.0 (Systat software Inc. San Jose, CA, USA).

4. RESULTS AND DISCUSSION

The organo-ceramic composite fibers of PCL and HA (1%, 5%, and 10%) were collected on a stationary target with random orientation. The presence of HA in the composite was confirmed by the peak centered at ca.1050 cm^{-1} in the FTIR scans as shown in Figure 1. It shows an increase in the intensity with increasing HA content. The additional peaks for phosphate groups of HA are at around 561 cm^{-1} and indicate a successive increase in the intensity with an increase in HA content in the composite fibers of the scaffold. Peak characteristic of the PCL are evident in the doublets centered at ca. 2950 cm^{-1}, which arise from C-H stretching, and the strong peak at ca. 1750 cm^{-1} is attributable to the ester group (COO) (Figure 1) (19). Previous studies have also demonstrated the use of FTIR for the characterization of HA composites (20, 21). In addition to this, hydroxyapatite from human fossils, hydroxyapatite-coated with titanium, combined with carbonated apatite, and carbon hydroxyapatite for bone tissue engineering have been characterized by FTIR spectroscopy (21-23). In the present investigation, we found that with increasing concentrations of HA in the organo-ceramic composites have different absorption patterns as compared to the control (Figure 1). These results are in agreement with the previous findings (21, 24, 25).

DSC is an effective analytical tool to characterize the physical properties of biphasic composite fibers and enables to determine the melting, crystallization, mesomorphic transition temperatures. It also highlights the corresponding enthalpy and entropy changes, characterize the glass transition and other effects related to changes in heat capacity. Thus, DSC was performed to study the aforementioned physical parameters of the composite fibers. DSC scans of composite fibers, Neat-PCL, and PCL/HA (1%, 5%, and 10%) showed their melting behaviors when DSC scans were obtained

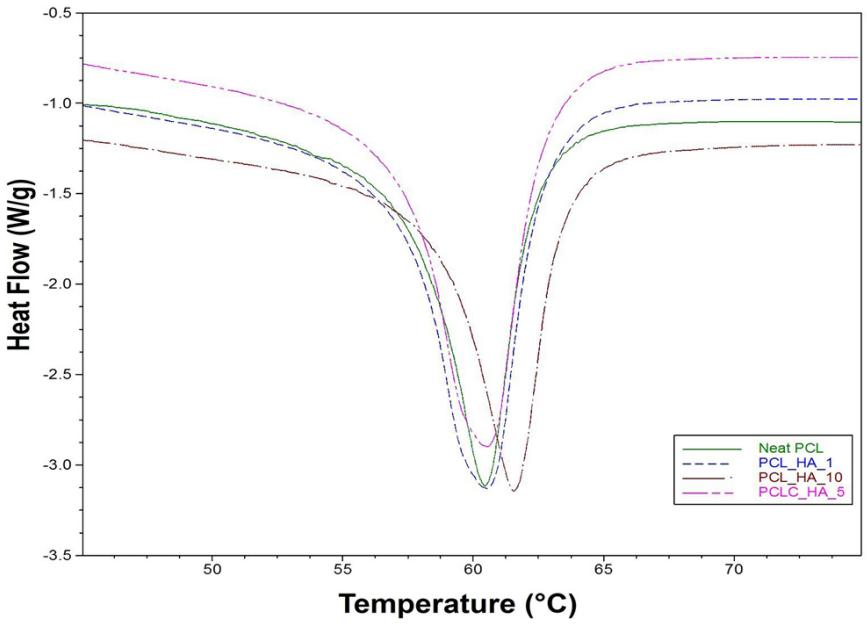

Figure 2. DSC scans of Neat-PCL and samples containing 1%, 5%, and 10% wt.% of HA. The DSC curves obtained at a heating rate of 10 °C per min to observe the effect of HA on the melting transition. The addition of HA up to 10% did not significantly affect the melting temperature of Neat-PCL around 60 °C.

(Figure 2). As a result of melting behavior, Neat-PCL showed a melting peak ca. 60.2 ^{0}C (Figure 2) (19). There is no obvious trend in the melting temperature or in the enthalpy of fusion associated with melting (Figure 2). Further analysis revealed that the DSC scan obtained from PCL/HA-1%, PCL/HA-5%, and PCL/HA-10% showed a melting peak at ca. 60.3 ^{0}C, ca. 60.5 ^{0}C, and ca. 61.1 ^{0}C respectively, which were different from Neat-PCL (Figure 2). These results are in agreement with the other studies (26, 27).

Scanning Electron Microscope (SEM) has been developed as a tremendous tool for the use in scientific and industrial applications. The high resolution SEM is especially useful for both quantitative and qualitative nanomanufacturing. In order to examine the structure/porosities of Neat-PCL, PCL/HA-1%, PCL/HA-5%, and PCL/HA-10% biphasic composite scaffolds, SEM was carried out. These results showed a structural difference in scaffolds when compared with the control groups (Figure 3). The composite fiber scaffolds showed a proportional relationship between increasing HA concentrations and fibers structural complexity (Figure 3). A scanning electron micrograph from a previously published study showed similar findings (28, 29). A higher porosity in PCL/HA scaffold was observed when compared to the Neat-PCL (Figure 3), which is in agreement with previous reports (30-32). In brief, higher HA (≥ 5% and 10%) promotes high porosity as compared to Neat-PCL (Figure 3).

The porosities of Neat-PCL, PCL/HA-1%, PCL/HA-5%, and PCL/HA-10% scaffolds were examined using SEM. Our results suggest that the porosity of PCL/HA scaffolds is HA concentration-dependent (Figure 3). These findings are in agreement with previously published studies (28, 29). A higher porosity in PCL/HA scaffolds was observed when compared to the Neat-PCL (Figure 3), which was also supported by other reports (30-32). Further analysis revealed that the application of 10% HA promotes high porosity as compared to Neat-PCL and 1% HA (Figure 3). These findings were compared to porosities calculated based on the apparent and bulk densities of the electrospun scaffolds and bulk PCL, respectively, which did not show significant variation among the samples. The porosities were 73% for the Neat-PLA, and 76, 75 and 77% for the 1%, 5% and 10% HA samples, respectively. There was a slight increase in porosity for the HA containing samples relative to pure PCL.

MTT assays were performed to demonstrate the effects of organo-ceramic composite fibers on the proliferation of hMSCs. The hMSCs seeded on nanocomposite PCL/HA scaffolds in 12-well plate and showed high proliferation in HA concentration-dependent manner as compared to Neat-PCL (Figure 4). Additionally, previous studies have demonstrated that PCL/HA-based scaffolds showed high proliferation and osteogenic differentiation in human

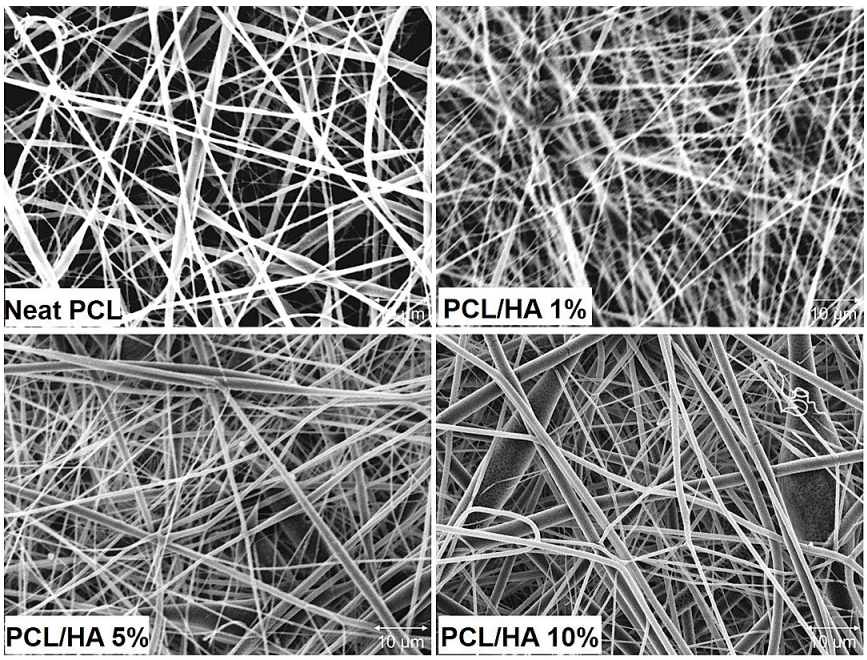

Figure 3. Scanning electron microphotographs (SEM) of Neat-PCL and PCL containing 1%, 5% and 10% wt.% of HA. Images obtained from SEM showing porosity of PCL/HA scaffolds. The addition of HA increased the porosity of the scaffolds and pore size which are important parameters for cellular growth. Moreover, the scaffolds exhibited a well-interconnected pore network structure irrespective of HA content in them.

dental pulp stem cells (hDPSCs) and mouse adipose-derived stem cells (ADSCs) (33, 34). Interestingly, magnetic bioinspired hybrid nanocomposite collagen-hydroxyapatite scaffolds enhanced cellular proliferation and restored bone generation (35, 36). However, the current study suggests that composites of PCL/HA-5% and PCL/HA-10% have a great impact on hMSCs proliferation as compared to Neat-PCL and PCL/HA-1% (Figure 4). Cell proliferation, cell cycle, and extracellular matrix are higher when hMSCs were exposed to HA (37, 38, 39, 40). We demonstrated that cellular proliferation was increased in an HA-concentration dependent manner when hMSCs were grown on PCL/HA composites, which is also in agreement with the other studies (41-43). PCL/HA and HA combined with other polymers incubated with stem cells showed a high rate of cell proliferation, osteogenic differentiation, and increased adhesion to surface (44-47).

The morphology and interconnection of cells were further examined using fluorescent microscopy (Figure 5). In Neat-PCL scaffold group, the cells proliferate but did not cover the entire strut surface of the scaffolds. Possibly these effects are due to the relatively low availability of HA scaffold surface area to attach cells (Figure 5). In contrast, on HA scaffolds (5% and 10%) group, the hMSCs spread completely and form confluent layer on the strut surface (Figure 5), suggesting the beneficial effects of PCL/HA biphasic composite scaffolds in governing cell morphology, growth, and proliferation (48). Cells incubated with 5% and 10% concentration of PCL/HA showed healthier cellular morphology as compared to Neat-PCL (Figure 5). In the previous reports, the morphology of electrospun nanofibrous scaffolds of segmented polyurethanes based on PEG, PLLA, and PTMC was determined using SEM (49, 50). Furthermore, the biocompatibility of highly microporous ceramic scaffolds was used to evaluate cell adhesion and morphology on scaffolds (51). No apoptotic cells were found when cells were observed under a fluorescent microscope after acridine orange (live cells produce green florescence) and propidium iodide (dead cells produce red fluorescence) staining (Figure 5).

To further examine the effects of different concentrations of HA (1%, 5%, and 10%) containing PCL on ECM cell adhesion molecule expression, the ECM cell adhesion assay (colorimetric) was carried out. We found that cells incubated with different concentrations (1%, 5%, and 10%) of HA showed increase expression of ECM cell adhesion molecules as compared to Neat-PCL (Figure 6). Additionally, results revealed that Collagen-I, II, and IV, modulated markedly as compared to Neat-PCL (Figure 6). Fibronectin, laminin, and vitronectin expression levels were also found significantly higher after 5% and 10% of PCL/HA exposure to hMSCs, suggesting that the organo-ceramic composite PCL/HA scaffolds are successful in mimicking the characteristics of natural bone (Figure 6). However, tenascin showed basal level expression in all experimental conditions (Figure 6). We found similar results when cells were analyzed

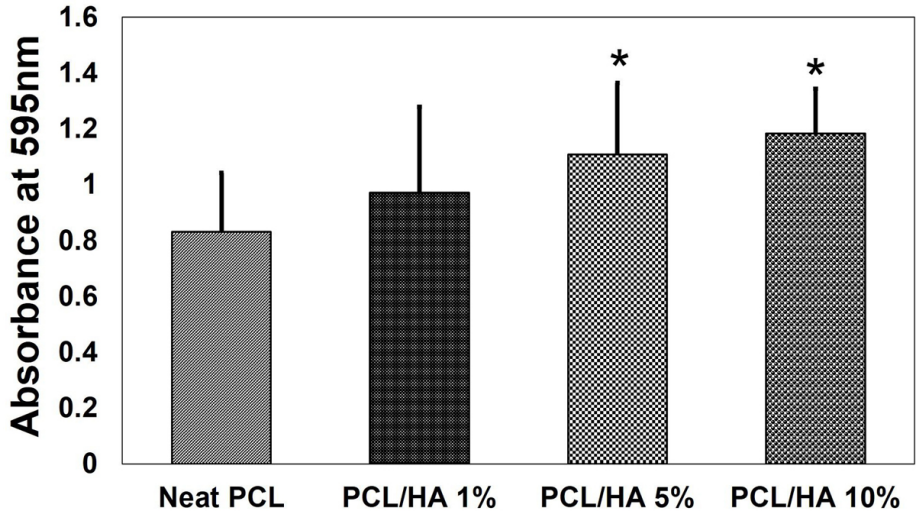

Figure 4. The hMSCs were grown on 1%, 5%, and 10% PCL/HA, and Neat-PCL in ATCC formulated culture medium for 48 h in 5% CO2 at 37 ^{0}C. After 48 h, to each well of microtiter plate 10µl of MTT (5mg/ml) was added and incubated for 4-5 h in the same environment. Further, to each well 100 µl of DMSO was added, and the plate was read at 595 nm using a microplate reader. The obtained histograms showed that 5% and 10% PCL/HA exposure to the hMSC cells increased cell proliferation as compared to Neat-PCL (* indicated p<0.0.5; control vs experimental).

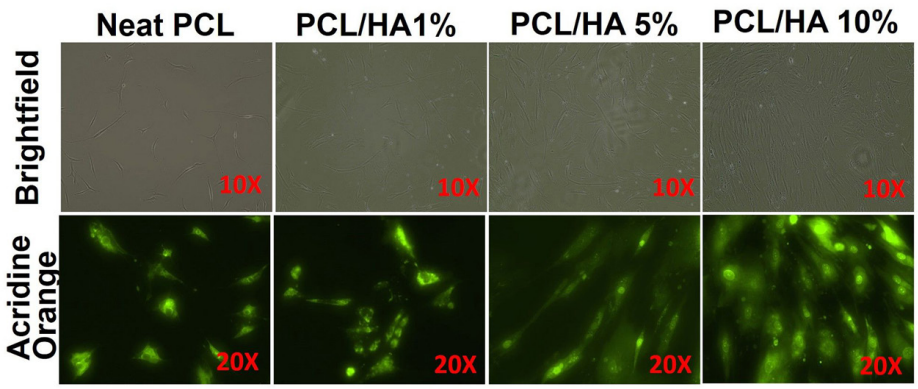

Figure 5. The hMSCs incubated with PCL containing 1%, 5% and 10% wt.% of HA in ATCC formulated culture medium supplemented with 7%, L-Alanyl-L-Glutamine, Insulin like Growth Factor-1, basic Fibroblast Growth Factor for 48 h in 5% CO2 at 37 ^{0}C. Cells were washed with DPBS and one set of cells were observed in phase contrast microscope while other sets of cells were observed under a fluorescence microscope after acridine orange and propidium iodide staining. Microscopic observations showed good cell morphology and no apoptotic/necrotic cell death.

morphologically, suggesting the contribution of PCL/HA nanocomposite scaffolds in the expression of ECM cell adhesion molecules, produced by hMSCs (Figure 6). These findings suggested that the exposure of different concentration (1%, 5%, and 10%) of HA modulates the expression of ECM cell adhesion molecules which ultimately contribute in enhancing the cell-cell, cell-scaffold interactions, cell spreading and thus survival of hMSCs on the composite surface. Early reports suggested that HA exposure to MC3T3-E1 cells showed enhanced the activity of ECM molecules on scaffolds (48, 52). PCL/HA scaffolds provide a natural environment to grow cells faster, which is similar to the growth pattern found in natural bone (48, 52). Furthermore, *in vivo* reports showed that HA treatment contributed to bone regeneration by modulating extracellular matrix production (53, 54). In addition, HA-scaffolds and porous HA-scaffolds influenced osteoblast cell proliferation and ECM molecule expression (37, 55). Results from the present investigation showed that the culture of hMSCs with PCL/HA nanocomposite scaffolds resulted in the high expression of ECM cell adhesion molecules, which further led to the increased expression of Collagen-I, II, and IV, fibronectin, laminin, and vitronectin (Figure 6) (56, 57). Our results showed that the organo-ceramic composite consist of 5% and 10% of HA induced cell-cell, cell-scaffold interactions, and the expression of ECM cell adhesion molecules. The biophasic composite scaffold efficiently mimics natural bones, and provide a great promise in bone tissue repair and regeneration (58-60).

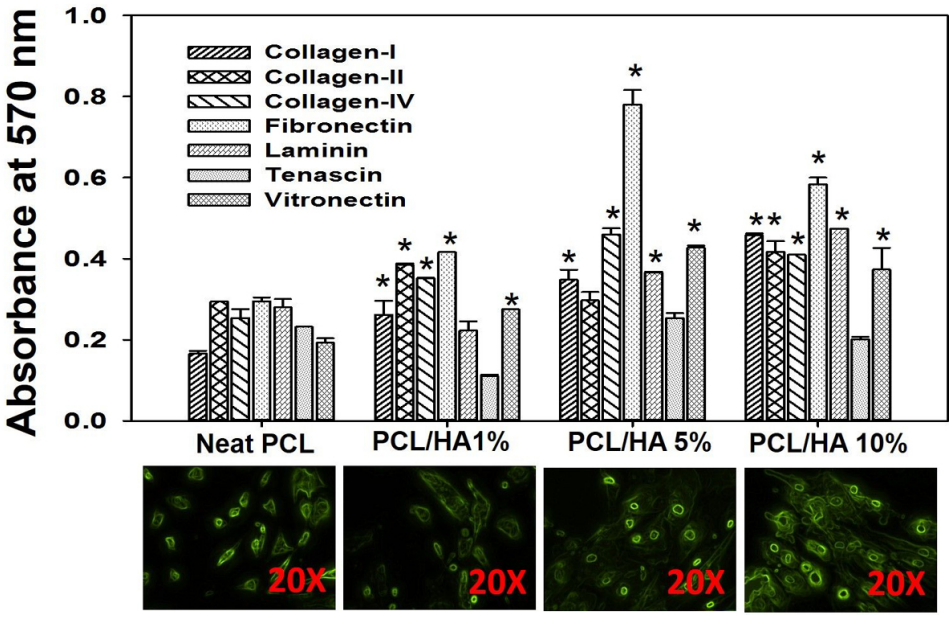

Figure 6. The hMSCs were grown on electrospun PCL/HA scaffolds for 48 h in 5% CO2 at 37 ^{0}C showed modulated expression of ECM cell adhesion molecule (collagen-I, II, IV, fibronectin, laminin, and vitronectin) as compared to the Neat-PCL. Similar results were obtained at the morphological ground when cells were analyzed morphologically ($p<0.05$; * indicated control vs experimental).

5. CONCLUSIONS

The application of organo-ceramic composite PCL/HA scaffolding to various fields of medical research continues to gain momentum each year. In this regard, we explored the impact of the biphasic composite PCL/HA scaffold with the primary attributes of a natural tissue, such as bone. PCL/HA scaffold provides a suitable natural bone environment for the efficient growth of hMSCs. The biological functionality was favorably regulated in terms of cell proliferation/ differentiation, cell adhesion, cell spreading, and the expression of ECM cell adhesion molecules and associated prominent protein such as collagens, fibronectin, laminin, and vitronectin.

PCL/HA scaffolds can be considered in natural bone grafting applications due in large part to its many cumulative benefits, which include various physio-mechanical properties and favorable biological activities. However, scaffold(s) morphology should be investigated further to improve cell adhesion to the surface of the polymer. Moreover, the present study offers a synthetic material for clinical use.

6. ACKNOWLEDGEMENTS

Sanjay Kumar performed biocompatibility experiments, analyzed data, and wrote the manuscript. Derrick Dean, Elijah Nyario and Christian Rogers prepared the biphasic organo-bioceramic fibrous composite. Vinoy Thomas performed porosity experiments, and edited the manuscript. James Stokes III critically reviewed the manuscript and helped in biological assays. Manoj K. Mishra conceived and designed the experiments, done a critical review of the manuscript, and provided infrastructure and research facility to performed aforementioned experiments. Authors do not have any conflict of interest. The authors have been fully supported US Department of Defense grants W911NF-12-1-0073 (Mishra, Dean, Nyairo and Thomas) and partially supported by National Institutes of Health grants P20CA192976 (Mishra); and W911NF-14-1-0064 (Mishra); National Science Foundation grants 1154214 (Mishra and Nyairo), and 1510479 (Dean, Mishra, and Nyairo).

7. REFERENCES

1. C Gao, Y Deng, P Feng, Z Mao, P Li, B Yang, J Deng, Y Cao, C Shuai, S Peng: Current progress in bioactive ceramic scaffolds for bone repair and regeneration. *Int J Mol Sci* 15, 4714-32 (2014) DOI: 10.3390/ijms15034714

2. RA Robinson: An electron-microscopic study of the crystalline inorganic component of bone and its relationship to the organic matrix. *J Bone Joint Surg Am* 34-A, 389-435; passim (1952)

3. JM Wilson, B Ashton, JT Triffitt: The interaction of a component of bone organic matrix with the mineral phase. *Calcif Tissue Res* 22 Suppl, 458-60 (1977)

4. MC Phipps, WC Clem, SA Catledge, Y Xu, KM Hennessy, V Thomas, MJ Jablonsky, S Chowdhury, AV Stanishevsky, YK Vohra, SL Bellis: Mesenchymal stem cell responses to bone-mimetic electrospun matrices composed of polycaprolactone, collagen I and nanoparticulate hydroxyapatite. *PLoS One* 6, e16813 (2011)

5. B Chuenjitkuntaworn, T Osathanon, N Nowwarote, P Supaphol, P Pavasant: The efficacy of polycaprolactone/hydroxyapatite scaffold in combination with mesenchymal stem cells for bone tissue engineering. *J Biomed Mater Res A* 104, 264-71 (2016)
DOI: 10.1002/jbm.a.35558

6. X Gao, J Song, P Ji, X Zhang, X Li, X Xu, M Wang, S Zhang, Y Deng, F Deng, S Wei: Polydopamine-Templated Hydroxyapatite Reinforced Polycaprolactone Composite Nanofibers with Enhanced Cytocompatibility and Osteogenesis for Bone Tissue Engineering. *ACS Appl Mater Interfaces* 8, 3499-515 (2016)
DOI: 10.1021/acsami.5b12413

7. E Prosecka, M Rampichova, A Litvinec, Z Tonar, M Kralickova, L Vojtova, P Kochova, M Plencner, M Buzgo, A Mickova, J Jancar, E Amler: Collagen/hydroxyapatite scaffold enriched with polycaprolactone nanofibers, thrombocyte-rich solution and mesenchymal stem cells promotes regeneration in large bone defect *in vivo*. *J Biomed Mater Res A* 103, 671-82 (2015)
DOI: 10.1002/jbm.a.35216

8. Q Yao, B Wei, N Liu, C Li, Y Guo, AN Shamie, J Chen, C Tang, C Jin, Y Xu, X Bian, X Zhang, L Wang: Chondrogenic regeneration using bone marrow clots and a porous polycaprolactone-hydroxyapatite scaffold by three-dimensional printing. *Tissue Eng Part A* 21, 1388-97 (2015)
DOI: 10.1089/ten.tea.2014.0280

9. B Dippel, RT Mueller, A Pingsmann, B Schrader: Composition, constitution, and interaction of bone with hydroxyapatite coatings determined by FT Raman microscopy. *Biospectroscopy* 4, 403-12 (1998)
DOI: 10.1002/(SICI)1520-6343(1998)4:6<403::AID-BSPY5>3.0.CO;2-M

10. RA Rozhnova, VI Bondarchuk, ES Savitskaia, EG Levenets, VA Popov, NA Galatenko: (Replacement of bone defects with a polyurethane composition with hydroxyapatite high-filling). *Lik Sprava* 1, 107-10 (2002)

11. R Arun Kumar, A Sivashanmugam, S Deepthi, S Iseki, KP Chennazhi, SV Nair, R Jayakumar: Injectable Chitin-Poly(epsilon-caprolactone)/Nanohydroxyapatite Composite Microgels Prepared by Simple Regeneration Technique for Bone Tissue Engineering. *ACS Appl Mater Interface*, 7, 9399-409 (2015)
DOI: 10.1021/acsami.5b02685

12. Y Luo, A Lode, C Wu, J Chang, M Gelinsky: Alginate/nanohydroxyapatite scaffolds with designed core/shell structures fabricated by 3D plotting and *in situ* mineralization for bone tissue engineering. *ACS Appl Mater Interfaces* 7, 6541-9 (2015)
DOI: 10.1021/am508469h

13. S Singh, AN Singh, A Verma, VK Dubey: Biodegradable polycaprolactone (PCL) nanosphere encapsulating superoxide dismutase and catalase enzymes. *Appl Biochem Biotechnol* 171, 1545-58 (2013)
DOI: 10.1007/s12010-013-0427-4

14. SS Henriksen, M Ding, MV Juhl, N Theilgaard, S Overgaard: Mechanical strength of ceramic scaffolds reinforced with biopolymers is comparable to that of human bone. *J Mater Sci Mater Med* 22, 1111-8 (2011)
DOI: 10.1007/s10856-011-4290-y

15. SI Roohani-Esfahani, P Newman, H Zreiqat: Design and Fabrication of 3D printed Scaffolds with a Mechanical Strength Comparable to Cortical Bone to Repair Large Bone Defects. *Sci Rep* 6, 19468 (2016)

16. MA Basile, GG d'Ayala, M Malinconico, P Laurienzo, J Coudane, B Nottelet, FD Ragione, A Oliva: Functionalized PCL/HA nanocomposites as microporous membranes for bone regeneration. *Mater Sci Eng C Mater Biol Appl* 48, 457-68 (2015)
DOI: 10.1016/j.msec.2014.12.019

17. LF Charles, MT Shaw, JR Olson, M Wei: Fabrication and mechanical properties of PLLA/PCL/HA composites via a biomimetic, dip coating, and hot compression procedure. *J Mater Sci Mater Med* 21, 1845-54 (2010)
DOI: 10.1007/s10856-010-4051-3

18. V Thomas, DR Dean, MV Jose, B Mathew, S Chowdhury, YK Vohra: Nanostructured

biocomposite scaffolds based on collagen coelectrospun with nanohydroxyapatite. *Biomacromolecules* 8, 631-7 (2007)
DOI: 10.1021/bm060879w

19. S Kumar, MS Tomar, A Acharya: Carboxylic group-induced synthesis and characterization of selenium nanoparticles and its anti-tumor potential on Dalton's lymphoma cells. *Colloids Surf B Biointerfaces* 126, 546-52 (2015)
DOI: 10.1016/j.colsurfb.2015.01.009

20. Y Huang, SG Han, QQ Ding, YJ Yan, XF Pang: (Preparation of chitosan/strontium-substituted hydroxyapatite films on titanium and its FTIR characteristics). *Guang Pu Xue Yu Guang Pu Fen Xi* 33, 2379-82 (2013)

21. H Ye, XY Liu, H Hong: Characterization of sintered titanium/hydroxyapatite biocomposite using FTIR spectroscopy. *J Mater Sci Mater Med* 20, 843-50 (2009)
DOI: 10.1007/s10856-008-3647-3

22. Y Huang, XF Pang, G Li, YJ Yan, SG Han, HJ Zeng: (Preparation of fluoridated hydroxyapatite coatings on titanium by electrolytic deposition and its FTIR characteristics). *Guang Pu Xue Yu Guang Pu Fen Xi* 32, 1771-4 (2012)

23. A Sroka-Bartnicka, JA Kimber, L Borkowski, M Pawlowska, I Polkowska, G Kalisz, A Belcarz, K Jozwiak, G Ginalska, SG Kazarian: The biocompatibility of carbon hydroxyapatite/beta-glucan composite for bone tissue engineering studied with Raman and FTIR spectroscopic imaging. *Anal Bioanal Chem* 407, 7775-85 (2015)
DOI: 10.1007/s00216-015-8943-4

24. AA Shaltout, MA Allam, MA Moharram: FTIR spectroscopic, thermal and XRD characterization of hydroxyapatite from new natural sources. *Spectrochim Acta A Mol Biomol Spectrosc* 83, 56-60 (2011)
DOI: 10.1016/j.saa.2011.07.036

25. D Verma, K Katti, D Katti: Experimental investigation of interfaces in hydroxyapatite/polyacrylic acid/polycaprolactone composites using photoacoustic FTIR spectroscopy. *J Biomed Mater Res A* 77, 59-66 (2006)
DOI: 10.1002/jbm.a.30592

26. HL Lai, K Pitt, DQ Craig: Characterisation of the thermal properties of ethylcellulose using differential scanning and quasi-isothermal calorimetric approaches. *Int J Pharm* 386, 178-84 (2010)
DOI: 10.1016/j.ijpharm.2009.11.013

27. S Pal, D Dasgupta: Differential scanning calorimetric approach to study the effect of melting region upon transcription initiation by T7 RNA polymerase and role of high affinity GTP binding. *J Biomol Struct Dyn* 31, 288-98 (2013)
DOI: 10.1080/07391102.2012.698237

28. T Lie: Early dental plaque morphogenesis. A scanning electron microscope study using the hydroxyapatite splint model and a low-sucrose diet. *J Periodontal Re*, 12, 73-89 (1977)
DOI: 10.1111/j.1600-0765.1977.tb00111.x

29. N Miura, K Kato: (Ultrastructural observation of sintered hydroxyapatite by scanning electron microscope). *Kokubyo Gakkai Zasshi*, 51, 172 (1984)

30. MV Jose, V Thomas, Y Xu, S Bellis, E Nyairo, D Dean: Aligned bioactive multi-component nanofibrous nanocomposite scaffolds for bone tissue engineering. *Macromol Biosci* 10, 433-44 (2010)
DOI: 10.1002/mabi.200900287

31. V Thomas, S Jagani, K Johnson, MV Jose, DR Dean, YK Vohra, E Nyairo: Electrospun bioactive nanocomposite scaffolds of polycaprolactone and nanohydroxyapatite for bone tissue engineering. *J Nanosci Nanotechnol* 6, 487-93 (2006)
DOI: 10.1166/jnn.2006.097

32. J Wang, CM Valmikinathan, W Liu, CT Laurencin, X Yu: Spiral-structured, nanofibrous, 3D scaffolds for bone tissue engineering. *J Biomed Mater Res A* 93, 753-62 (2010)

33. T Gao, N Zhang, Z Wang, Y Wang, Y Liu, Y Ito, P Zhang: Biodegradable Microcarriers of Poly(Lactide-co-Glycolide) and Nano-Hydroxyapatite Decorated with IGF-1 via Polydopamine Coating for Enhancing Cell Proliferation and Osteogenic Differentiation. *Macromol Biosci* 15, 1070-80 (2015)
DOI: 10.1002/mabi.201500069

34. A Khojasteh, SR Motamedian, MR Rad, MH Shahriari, N Nadjmi: Polymeric vs hydroxyapatite-based scaffolds on dental pulp stem cell proliferation and differentiation. *World J Stem Cells* 7, 1215-21 (2015)
DOI: 10.4252/wjsc.v7.i10.1215

35. M Esnaashary, M Fathi, M Ahmadian: *In vitro* evaluation of human osteoblast-like cell proliferation and attachment on nanostructured fluoridated hydroxyapatite. *Biotechnol Lett* 36, 1343-7 (2014)
DOI: 10.1007/s10529-014-1483-8

36. A Tampieri, M Iafisco, M Sandri, S Panseri, C Cunha, S Sprio, E Savini, M Uhlarz, T Herrmannsdorfer: Magnetic bioinspired hybrid nanostructured collagen-hydroxyapatite scaffolds supporting cell proliferation and tuning regenerative process. *ACS Appl Mater Interface*, 6, 15697-707 (2014)
DOI: 10.1021/am5050967

37. SH Cartmell, S Thurstan, JP Gittings, S Griffiths, CR Bowen, IG Turner: Polarization of porous hydroxyapatite scaffolds: influence on osteoblast cell proliferation and extracellular matrix production. *J Biomed Mater Res A* 102, 1047-52 (2014)
DOI: 10.1002/jbm.a.34790

38. F Li, J Peng, R Hu, X Dong, W Chen, Y Pan, X Tang, P Xie: Effect of nano-hydroxyapatite suspension on cell proliferation and cycle in human periodontal ligament cells. *J Nanosci Nanotechnol* 13, 4560-4 (2013)
DOI: 10.1166/jnn.2013.6704

39. E Prosecka, M Buzgo, M Rampichova, T Kocourek, P Kochova, L Vyslouzilova, D Tvrdik, M Jelinek, D Lukas, E Amler: Thin-layer hydroxyapatite deposition on a nanofiber surface stimulates mesenchymal stem cell proliferation and their differentiation into osteoblasts. *J Biomed Biotechnol* 2012, 428503 (2012)

40. M Wang, NJ Castro, J Li, M Keidar, LG Zhang: Greater osteoblast and mesenchymal stem cell adhesion and proliferation on titanium with hydrothermally treated nanocrystalline hydroxyapatite/magnetically treated carbon nanotubes. *J Nanosci Nanotechnol* 12, 7692-702 (2012)
DOI: 10.1166/jnn.2012.6624

41. L Cai, AS Guinn, S Wang: Exposed hydroxyapatite particles on the surface of photo-crosslinked nanocomposites for promoting MC3T3 cell proliferation and differentiation. *Acta Biomater* 7, 2185-99 (2011)
DOI: 10.1016/j.actbio.2011.01.034

42. J Xiong, Y Li, PD Hodgson, C Wen: *In vitro* osteoblast-like cell proliferation on nano-hydroxyapatite coatings with different morphologies on a titanium-niobium shape memory alloy. *J Biomed Mater Res A* 95, 766-73 (2010)
DOI: 10.1002/jbm.a.32903

43. D Kumar, JP Gittings, IG Turner, CR Bowen, LA Hidalgo-Bastida, SH Cartmell: Polarization of hydroxyapatite: influence on osteoblast cell proliferation. *Acta Biomater* 6, 1549-54 (2010)
DOI: 10.1016/j.actbio.2009.11.008

44. DD. Deligianni, ND Katsala, PG Koutsoukos, YF Missirlis: Effect of surface roughness of hydroxyapatite on human bone marrow cell adhesion, proliferation, differentiation and detachment strength. *Biomaterials* 22, 87-96 (2001)
DOI: 10.1016/S0142-9612(00)00174-5

45. T Higashi, H Okamoto: Influence of particle size of hydroxyapatite as a capping agent on cell proliferation of cultured fibroblasts. *J Endod* 22, 236-9 (1996)
DOI: 10.1016/S0099-2399(06)80139-1

46. T Iwakami, T Imai: Effect of hydroxyapatite sol on cell proliferation and alkaline phosphatase activity of osteoblastic MC3T3-E1 cells. *Biomed Mater Eng* 12, 249-57 (2002)

47. A Kasaj, B Willershausen, C Reichert, B Rohrig, R Smeets, M Schmidt: Ability of nanocrystalline hydroxyapatite paste to promote human periodontal ligament cell proliferation. *J Oral Sci* 50, 279-85 (2008)
DOI: 10.2334/josnusd.50.279

48. A Kumar, KC Nune, RD Misra: Biological functionality of extracellular matrix-ornamented three-dimensional printed hydroxyapatite scaffolds. *J Biomed Mater Res A* 104, 1343-51 (2016)
DOI: 10.1002/jbm.a.35664

49. RB. Trinca, GA Abraham, MI Felisberti: Electrospun nanofibrous scaffolds of segmented polyurethanes based on PEG, PLLA and PTMC blocks: Physico-chemical properties and morphology. *Mater Sci Eng C Mater Biol Appl* 56, 511-7 (2015)
DOI: 10.1016/j.msec.2015.07.018

50. M Ye, P Mohanty, G Ghosh: Morphology and properties of poly vinyl alcohol (PVA) scaffolds: impact of process variables. *Mater Sci Eng C Mater Biol Appl* 42, 289-94 (2014)
DOI: 10.1016/j.msec.2014.05.029

51. S Teixeira, MP Ferraz, FJ Monteiro: Biocompatibility of highly macroporous ceramic scaffolds: cell adhesion and morphology studies. *J Mater Sci Mater Med* 19, 855-9 (2008)
DOI: 10.1007/s10856-007-3005-x

52. N Jusoh, S Oh, S Kim, J Kim, NL Jeon: Microfluidic vascularized bone tissue model with hydroxyapatite-incorporated extracellular matrix. *Lab Chip* 15, 3984-8 (2015)
DOI: 10.1039/C5LC00698H

53. RD Ventura, AR Padalhin, YK Min, BT Lee: Bone Regeneration Using Hydroxyapatite Sponge Scaffolds with *In vivo* Deposited Extracellular Matrix. *Tissue Eng Part A* 21, 2649-61 (2015)
DOI: 10.1089/ten.tea.2015.0024

54. MM Villa, L Wang, DW Rowe, M Wei: Effects of cell-attachment and extracellular matrix on bone formation *in vivo* in collagen-hydroxyapatite scaffolds. *PLoS One* 9, e109568 (2014)

55. Y Wang, H Meng, X Yuan, J Peng, Q Guo, S Lu, A Wang: Fabrication and *in vitro* evaluation of an articular cartilage extracellular matrix-hydroxyapatite bilayered scaffold with low permeability for interface tissue engineering. *Biomed Eng Online* 13, 80 (2014)

56. W Kang, TI Kim, Y Yun, HW Kim, JH Jang: Engineering of a multi-functional extracellular matrix protein for immobilization to bone mineral hydroxyapatite. *Biotechnol Lett* 33, 199-204 (2011)
DOI: 10.1007/s10529-010-0412-8

57. W Song, DC Markel, S Wang, T Shi, G Mao, W Ren: Electrospun polyvinyl alcohol-collagen-hydroxyapatite nanofibers: a biomimetic extracellular matrix for osteoblastic cells. *Nanotechnology* 23, 115101 (2012)

58. PV Hauschka, FH Wians, Jr.: Osteocalcin-hydroxyapatite interaction in the extracellular organic matrix of bone. *Anat Rec* 224, 180-8 (1989)
DOI: 10.1002/ar.1092240208

59. E Pecheva, L Pramatarova, G. Altankov: Hydroxyapatite grown on a native extracellular matrix: initial interactions with human fibroblasts. *Langmuir* 23, 9386-92 (2007)
DOI: 10.1021/la700435c

60. L Pramatarova, E Pecheva, R Presker, MT Pham, MF Maitz, M Stutzmann: Hydroxyapatite growth induced by native extracellular matrix deposition on solid surfaces. *Eur Cell Mater* 9, 9-12 (2005)

Abbreviations: PCL: polycaprolactone, HA: hydroxyapatite, ECM: extracellular matrix, hMSC: human mesenchymal stem cell, MTT:(3-(4,5-dimethylthiazol-2-yl)-2,5diphenyltetrazolium bromide), DSC: Differential scanning calorimetry, FTIR: Fourier Transform Infrared Spectroscopy, FBS: fetal bovine serum

Key Words: PCL/HA scaffolds, Cell proliferation, ECM cell adhesion molecules, hMSC, Bone tissue engineering

Send correspondence to: Manoj K. Mishra, Cancer Biology Research and Training Program, Department of Biological Sciences, Alabama State University, 915 S Jackson Street, Montgomery, AL 36104, Tel: 314-229-5085, Fax: 334-229-5035, E-mail: mmishra@alasu.edu